



Title	Role of nucleocapsid protein of hantaviruses in intracellular traffic of viral glycoproteins
Author(s)	Shimizu, Kenta; Yoshimatsu, Kumiko; Koma, Takaaki; Yasuda, Shumpei P.; Arikawa, Jiro
Citation	Virus research, 178(2), 349-356 https://doi.org/10.1016/j.virusres.2013.09.022
Issue Date	2013-12-26
Doc URL	http://hdl.handle.net/2115/54732
Type	article (author version)
File Information	Virus Res_178(2)_349-356.pdf



[Instructions for use](#)

1 Research article

2

3 **Role of Nucleocapsid Protein of Hantaviruses in Intracellular Traffic of Viral**

4 **Glycoproteins**

5

6 Kenta Shimizu, Kumiko Yoshimatsu, Takaaki Koma, Shumpei P Yasuda, Jiro Arikawa*

7

8 Department of Microbiology, Hokkaido University Graduate School of Medicine,

9 Kita-15, Nishi-7, Kita-ku, Sapporo 060-8638, Japan.

10

11 *Corresponding author: Jiro Arikawa, Department of Microbiology, Hokkaido

12 University Graduate School of Medicine, Kita-15, Nishi-7, Kita-ku, Sapporo 060-8638,

13 Japan. Phone: +81-11-706-6905. Fax: +81-11-706-6905. E-mail:

14 j_arika@med.hokudai.ac.jp

15

16 **Summary**

17 To understand the role of nucleocapsid protein (NP) of hantaviruses in viral assembly,
18 the effect of NP on intracellular traffic of viral glycoproteins Gn and Gc was
19 investigated. Double staining of viral and host proteins in Hantaan virus
20 (HTNV)-infected Vero E6 cells showed that Gn and Gc were localized to cis-Golgi, in
21 which virus particles are thought to be formed. When HTNV Gn and Gc were expressed
22 by a plasmid encoding glycoprotein precursor (GPC), which is posttranslationally
23 cleaved into Gn and Gc, Gn was localized to cis-Golgi, whereas Gc showed diffuse
24 distribution in the cytoplasm in 32.9% of Gc-positive cells. The ratio of the diffused
25 Gc-positive cells was significantly decreased to 15.0% by co-expression of HTNV NP.
26 Co-expression of HTNV GPC with NPs of other hantaviruses, such as Seoul virus,
27 Puumala virus and Sin Nombre virus, also reduced the ratios of diffused Gc-positive
28 cells to 13.5%, 25.2%, and 11.6%, respectively. Among amino- and carboxyl-terminally
29 truncated HTNV NPs, NP75-429, NP116-429, NP1-333, NP1-233, and NP1-155
30 possessed activity to reduce the ratio of diffused Gc-positive cells, while NP155-429
31 and NP1-116 did not. NP30-429 has partial activity. These results indicate that amino
32 acid region 116-155 of NP is important for the activity, although amino acid region 1-30
33 is partially related. Truncation of the HTNV Gc cytoplasmic tail caused an increase in
34 diffused Gc-positive cells. In addition, the effect of coexpression of HTNV NP was
35 weakened. These results suggest that HTNV NP has a role to promote Golgi localization
36 of Gc through a mechanism possibly mediated by the Gc cytoplasmic tail.

37

38 **Keywords**

39 HFRS; HPS; Bunyaviridae; Assembly; Transport; Golgi

40

41 **1. Introduction**

42 Hantaviruses are classified into the family *Bunyaviridae*, genus *Hantavirus*.
43 Hantaviruses have been found in animals belonging to the Orders Rodentia,
44 Soricomorpha and Chiroptera. To date, only rodent-borne hantaviruses have been
45 thought to be pathogenic to humans. Hemorrhagic fever with renal syndrome (HFRS)
46 and hantavirus pulmonary syndrome (HPS) are severe diseases caused by infection of
47 hantaviruses. HFRS is characterized by renal dysfunction and hemorrhage and is caused
48 by Old World hantaviruses such as Hantaan virus (HTNV), Seoul virus (SEOV),
49 Dobrava virus (DOBV) and Puumala virus (PUUV). HPS is characterized by acute
50 respiratory distress and is caused by New World hantaviruses such as Sin Nombre virus
51 (SNV) and Andes virus (ANDV). The number of HFRS cases is estimated to be more
52 than 100,000 per year with a case-fatality rate of less than 10%. In contrast, although
53 the number of HPS cases is estimated to be only a few thousand per year, the
54 case-fatality rate of HPS has reached as high as 40%. Specific treatments and vaccines
55 against HFRS and HPS remain to be developed (Jonsson et al., 2010).

56 Hantaviruses are enveloped spherical or polymorphic viruses with a diameter of 80
57 to 120 nm. The genomes of hantaviruses are composed of tri-segmented single-stranded,
58 negative sense RNA, designated as small (S), medium (M) and large (L) segments.
59 Each segment encodes nucleocapsid protein (NP), glycoprotein precursor (GPC) and
60 RNA-dependent RNA polymerase (RdRp), respectively. GPC is posttranslationally
61 cleaved into Gn and Gc (Lober et al., 2001). NP is associated with the genome and is
62 involved in transcription, translation and replication together with RdRp (Mir et al.,
63 2008a, 2008b, 2010). Glycoproteins Gn and Gc are transmembrane proteins and
64 constitute an envelope with a lipid membrane derived from host cells. Gn and Gc are

65 involved in receptor binding, membrane fusion and induction of protective immunity
66 (Arikawa et al., 1992; Ogino et al., 2004; Ray et al., 2010). In some hantaviruses such
67 as Tula virus, PUUV, and ANDV, nonstructural protein (NSs) is also encoded in S
68 segment (Jaaskelainen et al., 2007; Vera-Otarola et al., 2011).

69 Formation of progeny particles of hantaviruses is thought to take place in the Golgi
70 complex as is the case in representative viruses of the Bunyaviridae family (Schmaljohn
71 and Nichol, 2007). However, the mechanism leading to assembly of viral components
72 remains unclear. In many other viruses, matrix protein has a key role in the process of
73 assembly and particle formation (Chen et al., 2008; Craven et al., 1999; Harty et al.,
74 2000). However, matrix protein is not encoded in the hantaviral genome, raising the
75 possibility that other viral protein has a role alternatively. Formation of virus-like
76 particles of HTNV was shown in both GPC and NP expressing cells (Li et al., 2010),
77 but not in GPC expressing cells, implying that NP has a role in particle formation.
78 Indeed, interaction between NP and cytoplasmic tails of Gn and Gc has been reported
79 (Hepojoki et al., 2010b). In addition, it was reported that NP is localized at endoplasmic
80 reticulum (ER)-Golgi intermediate compartment (ERGIC) prior to its movement to the
81 Golgi compartment and that inhibition of transport of NP to ERGIC resulted in
82 reduction of virus replication (Ramanathan et al., 2007). Taking into account these
83 findings, we hypothesized that NP has alternative role of matrix protein in the process
84 of assembly and particle formation. In this study, to elucidate the role of NP in viral
85 assembly, the effect of GPC and NP expression on their intracellular traffic was
86 investigated.

87

88 **2. Materials and Methods**

89 2.1. Cells and viruses

90 Vero E6 cells (CRL-1586; American Type Culture Collection) were maintained in
91 Eagle's minimum essential medium (Life Technologies) supplemented with 5% fetal
92 calf serum, 1% insulin-transferrin-selenium (Life Technologies) and 1% MEM
93 non-essential amino acids (Life Technologies). HTNV strain 76-118-derived clone-1
94 (Tamura et al., 1989), which was provided by Dr. K. Yamanishi (Osaka University
95 Medical School, Osaka, Japan), was propagated in Vero E6 cells.

96

97 2.2. Preparation of virus-infected cells

98 2×10^5 cells/ml of Vero E6 cells were mixed with a equal volume of medium
99 containing 2×10^3 focus-forming units (FFU)/ml of HTNV (multiplicity of infection =
100 0.01). 20 μ l of the mixture was seeded on 24-well 4 mm HTC slides (Thermo Scientific)
101 (2×10^3 cells/well). After incubation for 3 days, cells were fixed with 3%
102 paraformaldehyde in PBS for 10 min at room temperature and then permeabilized with
103 0.2% Triton X-100 in PBS for 4 min at room temperature.

104

105 2.3. Construction of plasmids

106 pCAGGS/MCS (Niwa et al., 1991) was used as a vector for expression of GPC and
107 NP in Vero E6 cells. pCHTNM and pCHTNS encoding GPC and NP of HTNV strain
108 76-118, and pCSEOS encoding NP of SEOV strain SR-11 were constructed previously
109 (Ogino et al., 2003; Yoshimatsu et al., 2003). pCPUUS encoding NP of PUUV strain
110 Kazan were constructed by digesting the pGEM-T-based plasmid including cDNA of
111 the NP gene of PUUV (Lundkvist et al., 1997) with *Sph*I and *Spe*I and cloning the

112 cDNA fragment into *SphI* and *NheI* sites of pCAGGS/MCS. pCSNS encoding NP of
113 SNV strain SN77734 was constructed by digesting the pFastBac-based plasmid
114 including cDNA of the NP gene of SNV (Koma et al., 2012) with *EcoRI* and *XhoI* and
115 cloning the cDNA fragment into pCAGGS/MCS. A series of amino and carboxyl
116 terminally-truncated HTNV NP expressing vectors, pCAGGS-HTNV-NP30-429,
117 pCAGGS-HTNV-NP75-429, pCAGGS-HTNV-NP116-429,
118 pCAGGS-HTNV-NP155-429, pCAGGS-HTNV-NP1-333, pCAGGS-HTNV-NP1-233,
119 pCAGGS-HTNV-NP1-155 and pCAGGS-HTNV-NP1-116, were constructed by
120 amplifying cDNA fragments with primers flanked by *EcoRI* and *XhoI* sites and cloning
121 into pCAGGS/MCS. For expression of NP Δ 35-74 lacking amino acid region 35-74 of
122 HTNV NP, pCAGGS-HTNV-NP Δ 35-74 was constructed by utilizing overlap extension
123 PCR (Higuchi et al., 1988). pCAGGS-HTNV-GPC-ZF1 and
124 pCAGGS-HTNV-GPC-ZF2 encoding HTNV GPC with mutations in CCHC-type zinc
125 finger motif 1 (H to Q and C to S at amino acid positions 561 and 565) and 2 (H to Q
126 and C to S at amino acid positions 587 and 591) in the Gn cytoplasmic tail, respectively,
127 was constructed by utilizing overlap extension PCR (Higuchi et al., 1988). Primers
128 flanked by *EcoRI* and *XhoI* sites and primers for introducing the mutations were used.
129 pCAGGS-HTNV-GPC- Δ Gc-3 and pCAGGS-HTNV-GPC- Δ Gc-6 encoding HTNV GPC
130 with 3 or 6 amino acid deletions in the carboxyl terminal region of the Gc cytoplasmic
131 tail, respectively, were constructed by amplifying cDNA fragments with primer
132 containing stop codon and *XhoI* site and then cloning into *HindIII* and *XhoI* sites of
133 pCHTNM. Primer sequences are available upon request.

134

135 2.4. Expression of recombinant proteins

136 Vero E6 cells on 24-well 4 mm HTC slides (Thermo Fisher Scientific Inc.) were
137 transfected with various combinations of pCAGGS-based plasmids using TransIT LT1
138 (Takara Bio Inc.) according to the manufacturer's instructions. After incubation for 24
139 hours, the cells were fixed and permeabilized as described in section 2.2.

140

141 2.5. Immunofluorescence assay

142 To stain Gn, Gc and NP, mouse monoclonal antibodies 3D5, 5B7 and E5G6
143 (Arikawa et al., 1989; Yoshimatsu et al., 1996) were used as primary antibodies,
144 respectively, and Alexa Fluor 488 goat anti-mouse IgG (Life Technologies) was used as
145 a secondary antibody. To stain ER and cis-Golgi, rabbit anti-Protein disulfide isomerase
146 (PDI) polyclonal antibodies (Sigma-Aldrich) and rabbit anti-Mannosidase II (Man II)
147 polyclonal antibodies (Merck KGaA) were used as primary antibodies, respectively, and
148 Alexa Fluor 594 goat anti-rabbit IgG (Life Technologies) was used as a secondary
149 antibody. Cells were incubated with primary antibodies at room temperature for 1 hour.
150 After washing with PBS three times, cells were incubated with secondary antibodies at
151 room temperature for 1 hour. After washing, slides were mounted with glycerol for
152 fluorescence microscopy (Merck KGaA) diluted with PBS (1:1), covered, and sealed
153 with clear nail polish. Fluorescence was observed using ECLIPSE E600 (Nikon) and
154 confocal laser microscopy system A1 (Nikon).

155

156 2.6. Evaluation of the effect of NP on diffuse localization of Gc

157 Ratio of diffused Gc-positive cells was determined by counting Gc-positive cells and
158 diffused Gc-positive cells in each well. The number of Gc-positive cells in each well
159 was more than 300.

160

161 2.7. Statistical analysis

162 Student's *t* test was used to determine statistical significance. *P* values of <0.05 were
163 considered statistically significant.

164

165 **3. Results**

166 3.1. Localization of Gn, Gc and NP of HTNV in infected cells

167 To determine the localization of Gn, Gc and NP of HTNV in infected cells, the viral
168 proteins and the cis-Golgi or ER markers were doubly stained with Alexa Fluor 488-
169 and Alexa Fluor 594-conjugated antibodies, respectively. Gn was stained with a
170 granular pattern and colocalized with the cis-Golgi marker but not with the ER marker
171 (Fig. 1). Similarly, Gc was colocalized with the cis-Golgi marker. On the other hand, NP
172 was also stained with a granular pattern but only partially colocalized with the cis-Golgi
173 marker. These results indicated that Gn and Gc were localized to cis-Golgi, while NP
174 was localized to cis-Golgi as well as other compartments in infected cells.

175

176 3.2. Localization of Gn, Gc and NP of HTNV in GPC or NP-expressing cells

177 To determine whether the localization of Gn, Gc and NP in GPC or NP-expressing
178 cells was the same as that in infected cells, Vero E6 cells were transfected with a HTNV
179 GPC or NP-expressing vector and their localization was analyzed in the same way.
180 Expressed GPC is posttranslationally cleaved into Gn and Gc. Most of Gn was localized
181 to cis-Golgi in GPC-expressing cells as in infected cells (Fig. 2 and Fig. 3A). In contrast,
182 some Gc showed diffuse distribution in the cytoplasm in GPC-expressing cells (Fig. 2
183 and Fig. 3A). The ratio of diffused Gc-positive cells among total Gc-positive cells was
184 32.9%. Diffused Gc was not observed in infected cells. NP was localized to the
185 cytoplasm diffusely in NP-expressing cells (Fig. 2B). Thus, the localization of Gc and
186 NP in GPC or NP-expressing cells was different from that in infected cells.

187

188 3.3. Effect of coexpression of GPC and NP of HTNV on their localization

189 To determine whether Gn, Gc and NP each affect their localization, Vero E6 cells
190 were co-transfected with HTNV GPC and NP-expressing vectors. Co-expression of NP
191 caused reduction of the ratio of diffused Gc-positive cells in a dose-dependent manner
192 (Fig. 3A and 3B). To show time course of the effect of NP, cells were examined at
193 15~48 hours post transfection. The ratio of diffused Gc-positive cells reached a plateau
194 level (12.9~14.9%) around 24 hours post-transfection, which was a significantly lower
195 level than that in cells without NP (Fig. 3C). These results indicate that NP has activity
196 to reduce the diffused localization of Gc. On the other hand, the localization of NP was
197 not affected by co-transfection of a GPC-expressing vector (data not shown). In later
198 experiments, cells were examined at 24 hours post-transfection.

199

200 3.4. Activity of NPs of SEOV, PUUV, and SNV to reduce diffused localization of 201 HTNV Gc

202 To determine whether the activity of NP to reduce diffused localization of Gc was
203 conserved among other representative hantaviruses, NPs of SEOV, PUUV and SNV
204 were co-expressed with HTNV GPC. NPs of SEOV and SNV caused reduction of the
205 ratio of diffused Gc-positive cells to 13.5% and 11.7%, respectively, which were
206 comparable with that in the case of HTNV NP (Fig. 4). PUUV NP also caused reduction
207 of the ratio of diffused Gc-positive cells to 25.2%, though the degree of reduction was
208 lower than others (Fig. 4). To confirm the expression level of NPs, NPs were stained by
209 immunofluorescence assay (Supplementary Fig. 1). Expression level of NP of PUUV
210 was relatively low compared to those of NPs of HTNV, SEOV and SNV. To examine
211 whether the low expression level of PUUV NP was related to the low activity to reduce
212 diffuse distribution of Gc, increasing amount of pCPUUS was cotransfected with

213 pCHTNM. As a result, the ratio of diffused Gc-positive cells was decreased in a
214 dose-dependent manner (Supplementary Fig. 2B), indicating that PUUV NP also has the
215 activity. Thus, despite the heterologous relationship between NP and GPC, each NP
216 reduced the ratio of diffused Gc-positive cells.

217

218 3.5. Amino acid region of HTNV NP that is important for activity to reduce diffused
219 localization of Gc

220 To determine the amino acid region of NP that is important for activity to reduce
221 diffused localization of Gc, a series of truncated NP-expressing vectors were transfected
222 with a GPC-expressing vector. In the case of amino-terminally truncated HTNV NPs,
223 NP155-429 did not reduce the ratio of diffused Gc-positive cells, while NP75-429 and
224 NP116-429 reduced the ratio of those cells as did whole NP (Fig. 5). NP30-429 showed
225 only a slight reduction of the ratio of diffused Gc-positive cells. In the case of
226 carboxyl-terminally truncated HTNV NPs, NP1-333, NP1-233 and NP1-155 reduced
227 the ratio of diffused Gc-positive cells, while NP1-116 did not (Fig. 5). When expression
228 vector of NP Δ 35-74 lacking amino acid region 35-74 was transfected, the ratio of
229 diffused Gc positive cells was reduced. To confirm the expression level of NPs, NPs
230 were stained by immunofluorescence assay (Supplementary Fig. 3). Expression level of
231 NP30-429, NP155-429, and NP1-233 were relatively low. To examine whether the low
232 expression level of NP30-429 and NP155-429 were related to the low or no activity to
233 reduce diffuse distribution of Gc, increasing amount of the expression plasmids of
234 NP30-429 and NP155-429 were transfected. As a result, slight reduction of the ratio of
235 diffused Gc-positive cells was observed in NP30-429 expressing cells (Supplementary
236 Fig. 2C). In contrast, the ratio of those cells was not changed in NP155-429 expressing

237 cells (Supplementary Fig. 2D). These results indicate that amino acid region 116-155 of
238 HTNV NP is important for activity to reduce diffused localization of Gc, although
239 amino acid region 1-30 is partially related.

240

241 3.6. Effect of mutations in HTNV Gn and Gc cytoplasmic tails on their localization

242 Glycoproteins Gn and Gc of hantaviruses are transmembrane proteins consisting of
243 an ectodomain, transmembrane domain and cytoplasmic tail and they form a hetero
244 complex. Considering the topology of NP and glycoproteins, NP may affect the
245 localization of Gc by binding to the cytoplasmic tails of Gn and Gc. To examine this
246 possibility, the effect of mutations in two CCHC-type zinc finger motifs in the HTNV
247 Gn cytoplasmic tail and the effect of deletions of short HTNV Gc cytoplasmic tail were
248 investigated. Both of the regions are thought to be important for the binding of NP to
249 cytoplasmic tails (Hepojoki et al., 2010b; Wang et al., 2010). ZF1 and ZF2 were
250 mutants with amino acid mutations in zinc finger motif 1 (H561Q and C565S) or 2
251 (H587Q and C591S), respectively. Δ Gc-3 and Δ Gc-6 were mutants with deletion of 3 or
252 6 amino acids in the carboxyl terminal of Gc cytoplasmic tail, respectively. Expression
253 levels of wt GPC, ZF1, ZF2, Δ Gc-3, and Δ Gc-6 were similar (Supplementary Fig. 4).
254 Ratio of diffused Gc-positive cells in ZF1 or ZF2 expressing cells were comparable
255 with that in wild type GPC expressing cells (Fig. 6). In contrast, deletion of 6 amino
256 acids in the carboxyl terminal of Gc cytoplasmic tail caused an increase in the ratio of
257 diffused Gc-positive cells in the absence of NP. In addition, the effect of coexpression of
258 NP was weakened in Δ Gc-6 expressing cells (Fig. 6). These results indicate that the
259 HTNV Gc cytoplasmic tail is important for efficient cis-Golgi localization of Gc.

260

261 **4. Discussion**

262 Particles of hantaviruses are thought to be formed in the Golgi complex (Schmaljohn
263 and Nichol, 2007). Therefore, Golgi localization of viral glycoproteins Gn and Gc
264 should be an important step for their life cycle. We showed that Gn and Gc were mainly
265 detected in cis-Golgi in HTNV-infected cells (Fig. 1). We speculate that the quantity of
266 Gn and Gc in ER is very small, since Gn and Gc are transported to Golgi complex
267 immediately after synthesis in ER. In contrast, when HTNV GPC was expressed by
268 transfection, Gc showed diffuse distribution in some cells (Fig. 2 and Fig. 3A),
269 indicating that factors other than GPC are involved in efficient Golgi localization of Gc.
270 In this study, we found that HTNV NP has a role in promoting the Golgi localization of
271 Gc.

272 Some studies have shown that Gn and Gc form a hetero complex (Antic et al., 1992;
273 Hepojoki et al., 2010a). It has been also reported that the presence of both Gn and Gc is
274 essential for their Golgi localization (Pensiero and Hay, 1992; Ruusala et al., 1992).
275 Based on the results of those studies, we speculate that formation of a hetero complex is
276 a prerequisite for their transport to the Golgi complex. Interestingly, Gn was localized to
277 cis-Golgi in GPC-expressing cells regardless of the presence of NP, suggesting that
278 formation of a hetero complex before transport to the Golgi complex is accomplished
279 without NP and that Gc may be dissociated from the hetero complex after transport to
280 the Golgi complex. Therefore, NP may play a role in increasing stability of the hetero
281 complex after transport to the Golgi complex.

282 The instability of Gc may be due to its short cytoplasmic domain. The cytoplasmic
283 domain of Gc consists of only 6 amino acids. Deletion of the cytoplasmic domain
284 resulted in an increase of diffused distribution of Gc. In addition, the deletion decreased

285 the effect of NP. It has been reported that NP interacts with the short cytoplasmic
286 domain of Gc (Hepojoki et al., 2010b). Therefore, NP may stabilize the hetero complex
287 through interaction with the Gc cytoplasmic domain.

288 Analysis of deletion mutants of HTNV NP showed that amino acid regions 1-30 and
289 116-155 in NP were important to promote Golgi localization of Gc. The amino acid
290 region 116-155 seemed to be more important for the activity, since NP30-429 caused
291 slight reduction of diffused localization of Gc. In addition, NP75-429 and NP116-429,
292 which lacked amino acid region 1-30, were still functional. In the amino-terminal region,
293 there was an intramolecular coiled-coil structure consisting of two alpha-helices (Wang
294 et al., 2008). Alpha-helices 1 and 2 were located in amino acid regions 1-34 and 39-74,
295 respectively. Deletion of amino acid region 1-30 may disrupt folding of the
296 amino-terminal region and interfere with the activity of NP to promote Golgi
297 localization of Gc. The amino acid region 116-155, especially 135-148, in NP was
298 relatively conserved among hantaviruses including Thottapalayam virus that is one of
299 the shrew-borne hantaviruses and genetically distant from rodent-borne hantaviruses
300 (Fig. 7). These conserved amino acids may have an important role in the mechanism.
301 Old and New World hantaviruses have evolved differences in their interaction with host
302 cell machinery as well as in pathogenesis. HTNV enters cells via clathrin-mediated
303 endocytosis, while ANDV entry is clathrin-independent (Ramanathan et al., 2008).
304 HTNV requires an intact microtubule network for replication, while ANDV requires
305 actin. However, in this study, we found that NPs of SEOV, PUUV and SNV exerted a
306 similar effect over HTNV glycoproteins, suggesting that the activity of NP may be a
307 primitive feature common to hantaviruses. In other members of the *Bunyaviridae* family,
308 importance of cytoplasmic tails of the glycoproteins in viral assembly has been reported.

309 Shi et al. showed that the cytoplasmic tails of both Gn and Gc of Bunyamwera virus,
310 member of the *Orthobunyavirus* genus, play crucial role in virus assembly and
311 morphogenesis. The cytoplasmic tail of glycoprotein G_N of Uukuniemi virus, member
312 of the *Phlebovirus* genus, is important for Golgi retention, binding of nucleoprotein,
313 and genome packaging (Andersson et al., 1997; Overby et al., 2007). Overby et al.
314 showed the importance of a lysine at position -3 from the C terminus of the short
315 cytoplasmic tail of Uukuniemi virus G_C in Golgi localization and particle formation.
316 Interestingly, the lysine is highly conserved among members of the *Phlebovirus*,
317 *Hantavirus*, and *Orthobunyavirus* genera. In this study, we showed that the short
318 cytoplasmic tail of Gc is important for the correct localization of Gc and for receiving
319 support from NP. Considering these reports and findings, interaction between the
320 cytoplasmic tails of glycoproteins and nucleoprotein may be conserved feature for the
321 *Bunyaviridae* family that lacks matrix protein.

322

323 **Acknowledgements**

324 We are grateful to the Nikon Imaging Center at Hokkaido University for assistance
325 with confocal microscopy, image acquisition, and analysis. This study was supported in
326 part by the Program of Founding Research Centers for Emerging and Reemerging
327 Infectious Diseases, MEXT, Japan, a grant from the Global COE Program
328 (Establishment of International Collaboration Center for Zoonosis Control), and
329 Grants-in-Aid for Scientific Research from the Ministry of Education, Culture, Sports,
330 Science and Technology, Japan.

331

332 **References**

- 333 Andersson, A.M., Melin, L., Bean, A., Pettersson, R.F., 1997. A retention signal
334 necessary and sufficient for Golgi localization maps to the cytoplasmic tail of a
335 Bunyaviridae (Uukuniemi virus) membrane glycoprotein. *J. Virol.* 71,
336 4717-4727.
- 337 Antic, D., Wright, K.E., Kang, C.Y., 1992. Maturation of Hantaan virus glycoproteins
338 G1 and G2. *Virology* 189, 324-328.
- 339 Arikawa, J., Schmaljohn, A.L., Dalrymple, J.M., Schmaljohn, C.S., 1989.
340 Characterization of Hantaan virus envelope glycoprotein antigenic determinants
341 defined by monoclonal antibodies. *J. Gen. Virol.* 70, 615-624.
- 342 Arikawa, J., Yao, J.S., Yoshimatsu, K., Takashima, I., Hashimoto, N., 1992. Protective
343 role of antigenic sites on the envelope protein of Hantaan virus defined by
344 monoclonal antibodies. *Arch. Virol.* 126, 271-281.
- 345 Chen, B.J., Leser, G.P., Jackson, D., Lamb, R.A., 2008. The influenza virus M2 protein
346 cytoplasmic tail interacts with the M1 protein and influences virus assembly at
347 the site of virus budding. *J. Virol.* 82, 10059-10070.
- 348 Craven, R.C., Harty, R.N., Paragas, J., Palese, P., Wills, J.W., 1999. Late domain
349 function identified in the vesicular stomatitis virus M protein by use of
350 rhabdovirus-retrovirus chimeras. *J. Virol.* 73, 3359-3365.
- 351 Harty, R.N., Brown, M.E., Wang, G., Huibregtse, J., Hayes, F.P., 2000. A PPxY motif
352 within the VP40 protein of Ebola virus interacts physically and functionally with
353 a ubiquitin ligase: implications for filovirus budding. *Proc. Natl. Acad. Sci. USA*
354 97, 13871-13876.
- 355 Hepojoki, J., Strandin, T., Vaheri, A., Lankinen, H., 2010a. Interactions and

356 oligomerization of hantavirus glycoproteins. *J. Virol.* 84, 227-242.

357 Hepojoki, J., Strandin, T., Wang, H., Vapalahti, O., Vaheiri, A., Lankinen, H., 2010b.

358 Cytoplasmic tails of hantavirus glycoproteins interact with the nucleocapsid
359 protein. *J. Gen. Virol.* 91, 2341-2350.

360 Higuchi, R., Krummel, B., Saiki, R.K., 1988. A general method of in vitro preparation
361 and specific mutagenesis of DNA fragments: study of protein and DNA
362 interactions. *Nucleic Acids Res.* 16, 7351-7367.

363 Jaaskelainen, K.M., Kaukinen, P., Minskaya, E.S., Plyusnina, A., Vapalahti, O., Elliott,
364 R.M., Weber, F., Vaheiri, A., Plyusnin, A., 2007. Tula and Puumala hantavirus
365 NSs ORFs are functional and the products inhibit activation of the
366 interferon-beta promoter. *J. Med. Virol.* 79, 1527-1536.

367 Jonsson, C.B., Figueiredo, L.T., Vapalahti, O., 2010. A global perspective on hantavirus
368 ecology, epidemiology, and disease. *Clin. Microbiol. Rev.* 23, 412-441.

369 Koma, T., Yoshimatsu, K., Taruishi, M., Miyashita, D., Endo, R., Shimizu, K., Yasuda,
370 S.P., Amada, T., Seto, T., Murata, R., Yoshida, H., Kariwa, H., Takashima, I.,
371 Arikawa, J., 2012. Development of a serotyping enzyme-linked immunosorbent
372 assay system based on recombinant truncated hantavirus nucleocapsid proteins
373 for new world hantavirus infection. *J. Virol. Methods* 185, 74-81.

374 Li, C., Liu, F., Liang, M., Zhang, Q., Wang, X., Wang, T., Li, J., Li, D., 2010.

375 Hantavirus-like particles generated in CHO cells induce specific immune
376 responses in C57BL/6 mice. *Vaccine* 28, 4294-4300.

377 Lober, C., Anheier, B., Lindow, S., Klenk, H.D., Feldmann, H., 2001. The Hantaan virus
378 glycoprotein precursor is cleaved at the conserved pentapeptide WAASA.
379 *Virology* 289, 224-229.

380 Lundkvist, A., Cheng, Y., Sjolander, K.B., Niklasson, B., Vaheri, A., Plyusnin, A., 1997.
381 Cell culture adaptation of Puumala hantavirus changes the infectivity for its
382 natural reservoir, *Clethrionomys glareolus*, and leads to accumulation of mutants
383 with altered genomic RNA S segment. *J. Virol.* 71, 9515-9523.

384 Mir, M.A., and Panganiban, A.T., 2008a. A protein that replaces the entire cellular
385 eIF4F complex. *EMBO J.* 27, 3129-3139.

386 Mir, M.A., Duran, W.A., Hjelle, B.L., Ye, C., Panganiban, A.T., 2008b. Storage of
387 cellular 5' mRNA caps in P bodies for viral cap-snatching. *Proc. Natl. Acad. Sci.*
388 USA 105, 19294-19299.

389 Mir, M.A., Sheema, S., Haseeb, A., Haque, A., 2010. Hantavirus nucleocapsid protein
390 has distinct m7G cap- and RNA-binding sites. *J. Biol. Chem.* 285, 11357-11368.

391 Niwa, H., Yamamura, K., Miyazaki, J., 1991. Efficient selection for high-expression
392 transfectants with a novel eukaryotic vector. *Gene* 108, 193-199.

393 Ogino, M., Ebihara, H., Lee, B.H., Araki, K., Lundkvist, A., Kawaoka, Y., Yoshimatsu,
394 K., Arikawa, J., 2003. Use of vesicular stomatitis virus pseudotypes bearing
395 hantaan or seoul virus envelope proteins in a rapid and safe neutralization test.
396 *Clin. Diagn. Lab. Immunol.* 10, 154-160.

397 Ogino, M., Yoshimatsu, K., Ebihara, H., Araki, K., Lee, B.H., Okumura, M., Arikawa, J.,
398 2004. Cell fusion activities of Hantaan virus envelope glycoproteins. *J. Virol.* 78,
399 10776-10782.

400 Overby, A.K., Pettersson, R.F., Neve, E.P.A., 2007a. The glycoprotein cytoplasmic tail
401 of Uukuniemi virus (Bunyaviridae) interacts with ribonucleoproteins and is
402 critical for genome packaging. *J. Virol.* 81, 3198-3205.

403 Overby, A.K., Popov, V.L., Pettersson, R.F., Neve, E.P.A., 2007b. The cytoplasmic tails

404 of Uukuniemi virus (Bunyaviridae) GN and GC glycoproteins are important for
405 intracellular targeting and the budding of virus-like particles. *J. Virol.* 81,
406 11381-11391.

407 Pensiero, M.N. and Hay, J. (1992) The Hantaan virus M-segment glycoproteins G1 and
408 G2 can be expressed independently. *J Virol* 66(4), 1907-14.

409 Ramanathan, H.N., Chung, D.H., Plane, S.J., Sztul, E., Chu, Y.K., Guttieri, M.C.,
410 McDowell, M., Ali, G., Jonsson, C.B., 2007. Dynein-dependent transport of the
411 Hantaan virus nucleocapsid protein to the endoplasmic reticulum-Golgi
412 intermediate compartment. *J. Virol.* 81, 8634-8647.

413 Ramanathan, H.N. and Jonsson, C.B., 2008. New and Old World hantaviruses
414 differentially utilize host cytoskeletal components during their life cycles.
415 *Virology* 374, 138-150.

416 Ray, N., Whidby, J., Stewart, S., Hooper, J.W., Bertolotti-Ciarlet, A., 2010. Study of
417 Andes virus entry and neutralization using a pseudovirion system. *J. Virol.*
418 *Methods* 163, 416-423.

419 Ruusala, A., Persson, R., Schmaljohn, C.S. and Pettersson, R.F. (1992) Coexpression of
420 the membrane glycoproteins G1 and G2 of Hantaan virus is required for
421 targeting to the Golgi complex. *Virology* 186(1), 53-64.

422 Schmaljohn, C.S., Nichol, S.T., 2007. Bunyaviridae, in: Knipe, D.M., Howley, P.M.
423 (Eds.), *Fields Virology*. Lippincott Williams & Wilkins, Philadelphia, pp.
424 1741-1789.

425 Shi, X., Kohl, A., Li, P., Elliott, R.M., 2007. Role of the cytoplasmic tail domains of
426 Bunyamwera orthobunyavirus glycoproteins Gn and Gc in virus assembly and
427 morphogenesis. *J. Virol.* 81, 10151-10160.

428 Tamura, M., Asada, H., Kondo, K., Tanishita, O., Kurata, T., Yamanishi, K., 1989.
429 Pathogenesis of Hantaan virus in mice. *J. Gen. Virol.* 70, 2897-2906.

430 Vera-Otarola, J., Solis, L., Soto-Rifo, R., Ricci, E.P., Pino, K., Tischler, N.D., Ohlmann,
431 T., Darlix, J.L., Lopez-Lastra, M., 2012. The Andes hantavirus NSs protein is
432 expressed from the viral small mRNA by a leaky scanning mechanism. *J. Virol.*
433 86, 2176-2187.

434 Wang, H., Alminait, A., Vaheri, A., Plyusnin, A., 2010. Interaction between hantaviral
435 nucleocapsid protein and the cytoplasmic tail of surface glycoprotein Gn. *Virus*
436 *Res.* 151, 205-212.

437 Wang, Y., Boudreaux, D.M., Estrada, D.F., Egan, C.W., St Jeor, S.C., De Guzman, R.N.,
438 2008. NMR structure of the N-terminal coiled coil domain of the Andes
439 hantavirus nucleocapsid protein. *J. Biol. Chem.* 283, 28297-28304.

440 Yoshimatsu, K., Arikawa, J., Tamura, M., Yoshida, R., Lundkvist, A., Niklasson, B.,
441 Kariwa, H., Azuma, I., 1996. Characterization of the nucleocapsid protein of
442 Hantaan virus strain 76-118 using monoclonal antibodies. *J. Gen. Virol.* 77,
443 695-704.

444 Yoshimatsu, K., Lee, B.H., Araki, K., Morimatsu, M., Ogino, M., Ebihara, H., Arikawa,
445 J., 2003. The multimerization of hantavirus nucleocapsid protein depends on
446 type-specific epitopes. *J. Virol.* 77, 943-952.

447

448 **Legends to figures**

449 **Fig. 1.** Viral glycoproteins Gn and Gc were localized to cis-Golgi in HTNV-infected
450 Vero E6 cells. (A) Localization of viral proteins (left column) and ER marker (center
451 column). (B) Localization of viral proteins (left column) and cis-Golgi marker (center
452 column). Right columns show merged images. Mouse monoclonal antibodies 3D5, 5B7,
453 and E5G6 were used as primary antibodies for staining of Gn, Gc, and NP, respectively.
454 Rabbit anti-PDI polyclonal antibodies and rabbit anti-Man II polyclonal antibodies were
455 used as primary antibodies for staining of ER and cis-Golgi markers, respectively. Alexa
456 Fluor 488 goat anti-mouse IgG and Alexa Fluor 594 goat anti-rabbit IgG were used as
457 secondary antibodies.

458

459 **Fig. 2.** Appearance of diffused Gc in HTNV GPC-expressing cells. (A) Localization of
460 Gn, Gc (left column) and cis-Golgi marker (center column) in HTNV GPC-expressing
461 Vero E6 cells. (B) Localization of NP (left) and cis-Golgi marker (center) in HTNV
462 NP-expressing Vero E6 cells. Right columns show merged images. Vero E6 cells were
463 transfected with 30 ng/well of pCAGGS/MCS and 30ng/well of pCHTNM or pCHTNS.
464 After 24 hours, cells were fixed, stained and examined under microscope.

465

466 **Fig. 3.** Co-expression of HTNV GPC and NP promoted cis-Golgi localization of Gc.
467 (A) Localization of Gn and Gc in cells transfected with 30 ng/well of pCHTNM and 30
468 ng/well of pCAGGS/MCS (left column) or pCHTNS (right column) at 24 hours post
469 transfection. (B) Dose-dependent effect of NP on localization of Gc. Vero E6 cells were
470 co-transfected with pCHTNM (40 ng/well) and increasing amounts of pCHTNS. After
471 incubation for 24 hours, ratios of diffused Gc-positive cells were determined by

472 counting Gc- and diffused Gc-positive cells. (C) Time course of the ratio of diffused
473 Gc-positive cells. Vero E6 cells were co-transfected with 30 ng/well of pCHTNM and
474 30 ng/well of pCAGGS/MCS (open bar) or pCHTNS (filled bar) and incubated for
475 indicated periods. Error bars represent standard deviation of values determined by three
476 independent experiments.

477

478 **Fig. 4.** Co-expression of GPC of HTNV and NP of HTNV, SEOV, PUUV or SNV
479 promoted cis-Golgi localization of Gc. Vero E6 cells were co-transfected with 30
480 ng/well of pCHTNM and 30 ng/well of pCAGGS/MCS, pCHTNS, pCSEOS, pCPUUS
481 or pCSNS and incubated for 24 hours. Error bars represent standard deviation of values
482 determined by three independent experiments. Asterisks indicate significant differences
483 between empty and each NP expressing plasmid. * $p < 0.05$. ** $p < 0.01$.

484

485 **Fig. 5.** Identification of the amino acid region in NP that is important for activity to
486 reduce diffuse localization of Gc. Vero E6 cells were co-transfected with 30 ng/well of
487 pCHTNM and 30 ng/well of pCAGGS/MCS, pCHTNS or pCAGGS-based truncated
488 HTNV NP-expressing plasmids and incubated for 24 hours. The bars on the left of the
489 graph are pictorial representations of the portions of truncated NPs. Error bars represent
490 standard deviation of values determined by three independent experiments. Asterisks
491 indicate significant differences between empty and each NP expressing plasmid.

492 * $p < 0.05$. ** $p < 0.01$.

493

494 **Fig. 6.** Effect of Gn and Gc cytoplasmic tail mutations on localization of Gc. Vero E6
495 cells were co-transfected with 30 ng/well of pCAGGS-based wild type (wt) or mutant

496 HTNV GPC-expressing plasmids and 30 ng/well of pCAGGS/MCS (open bar) or
497 pCHTNS (filled bar) and incubated for 24 hours. Error bars represent standard deviation
498 of values determined by three independent experiments. Asterisks indicate significant
499 differences. * $p < 0.05$. ** $p < 0.01$.

500

501 **Fig. 7.** Alignment of partial amino acid sequences of NPs of representative hantaviruses.

502 Asterisks indicate conserved amino acid residues.

503

504 **Legends to Supplementary figures**

505 **Supplementary Fig. 1.** Expression level of NP in Vero E6 cells transfected with 30
506 ng/well of pCHTNM and 30 ng/well of pCHTNS, pCSEOS, pCPUUS or pCSNS at 24
507 hours post transfection. Mouse monoclonal antibody E5G6 and Alexa Fluor 488 goat
508 anti mouse IgG were used for staining of NP.

509

510 **Supplementary Fig. 2.** Dose-dependent effect of HTNV NP (A), PUUV NP (B),
511 HTNV NP30-429 (C) and HTNV NP155-429 (D) on localization of Gc. Vero E6 cells
512 were transfected with 20 ng/well of pCHTNM and increasing amount of pCHTNS,
513 pCPUUS, pCAGGS-HTNV-NP30-429 or pCAGGS-HTNV-NP155-429. After
514 incubation for 24 hours, ratios of diffused Gc-positive cells were determined by
515 counting Gc- and diffused Gc-positive cells. Error bars represent standard deviation of
516 values determined by three independent experiments. Asterisks indicate significant
517 differences between empty and each quantity of NP expressing plasmid. * $p < 0.05$.
518 ** $p < 0.01$.

519

520 **Supplementary Fig. 3.** Expression level of NP in Vero E6 cells transfected with 30
521 ng/well of pCHTNM and 30 ng/well of pCAGGS-based truncated HTNV
522 NP-expressing plasmids at 24 hours post transfection. Mouse monoclonal antibody
523 E5G6 was used for staining of NPs except for NP1-155 and NP1-116. Mouse
524 monoclonal antibody ECO2 was used for staining of NP1-155 and NP1-116. Alexa
525 Fluor 488 goat anti mouse IgG was used as secondary antibody.

526

527 **Supplementary Fig. 4.** Expression level of Gc in Vero E6 cells transfected with 30

528 ng/well of pCAGGS-based wild type (wt) or mutant HTNV GPC-expressing plasmids
529 and 30 ng/well of pCAGGS/MCS at 24 hours post transfection. Mouse monoclonal
530 antibody 5B7 and Alexa Fluor 488 goat anti mouse IgG were used for staining of Gc.
531

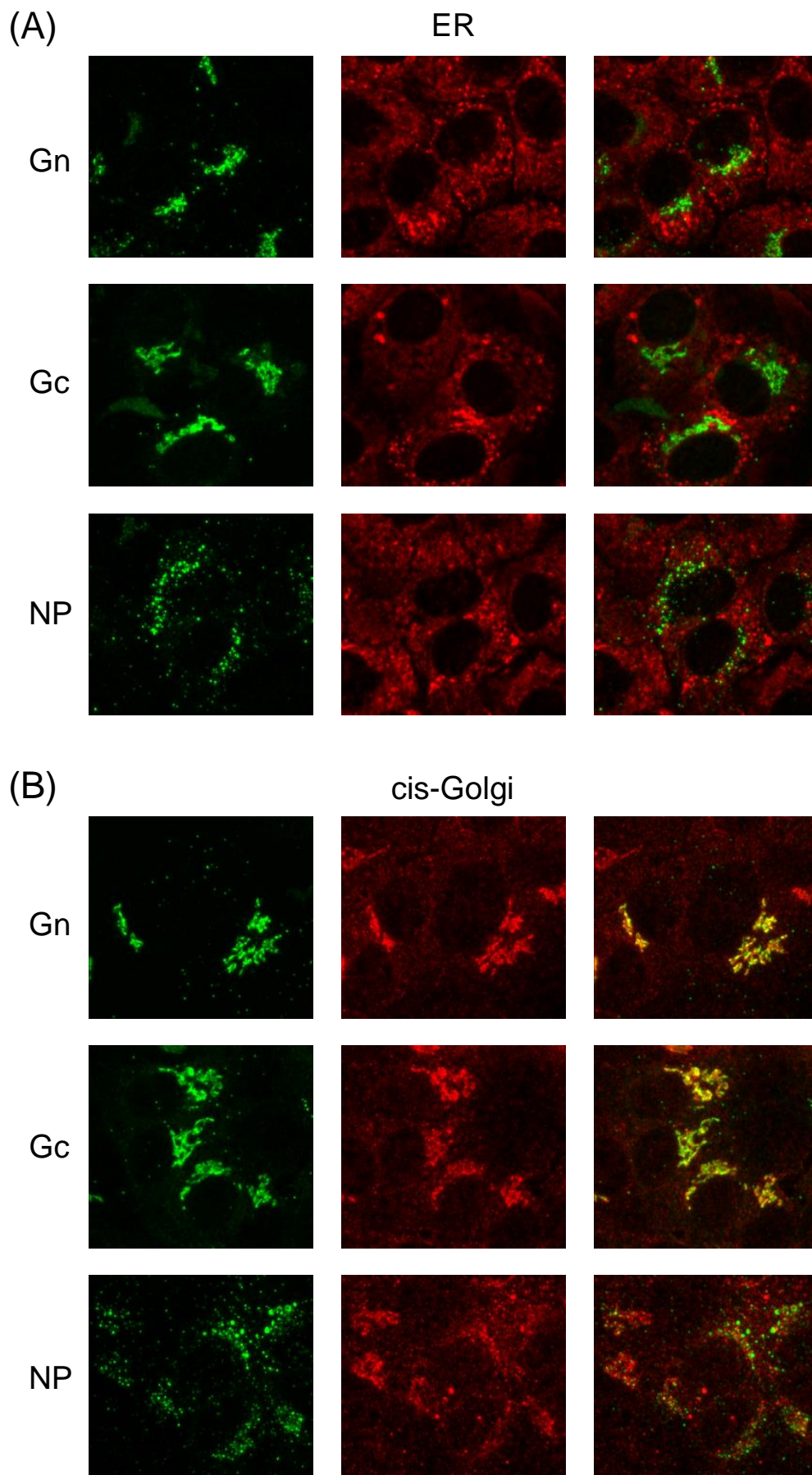


Fig. 1

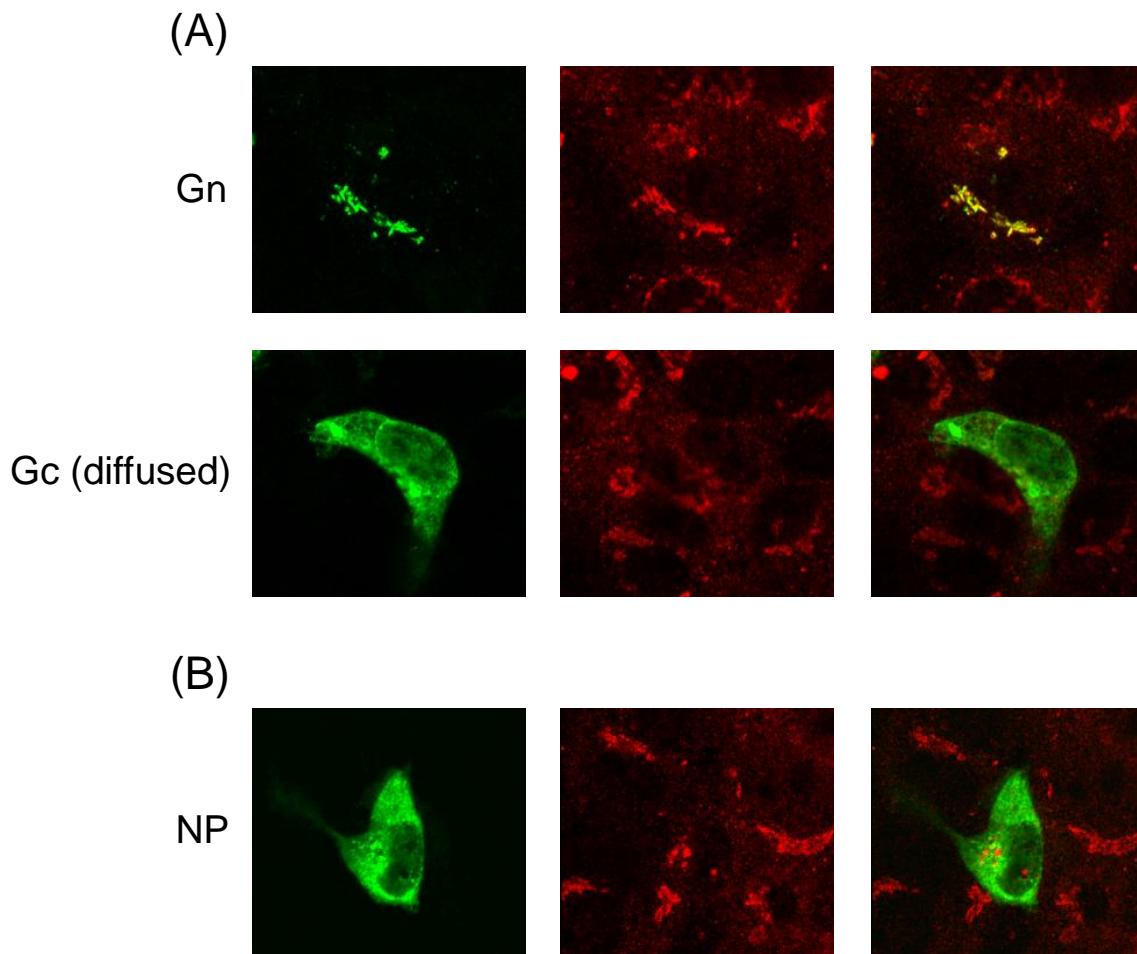


Fig. 2

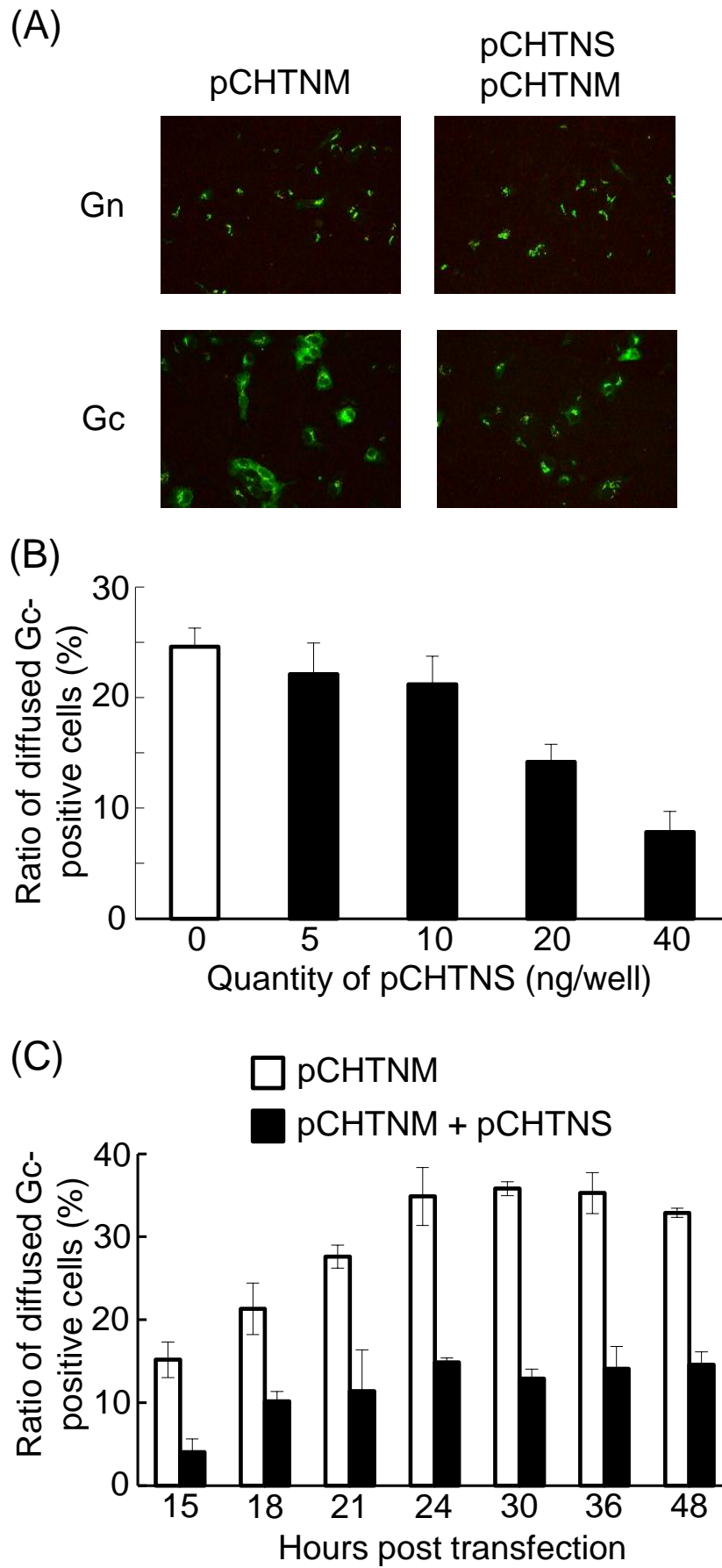


Fig. 3

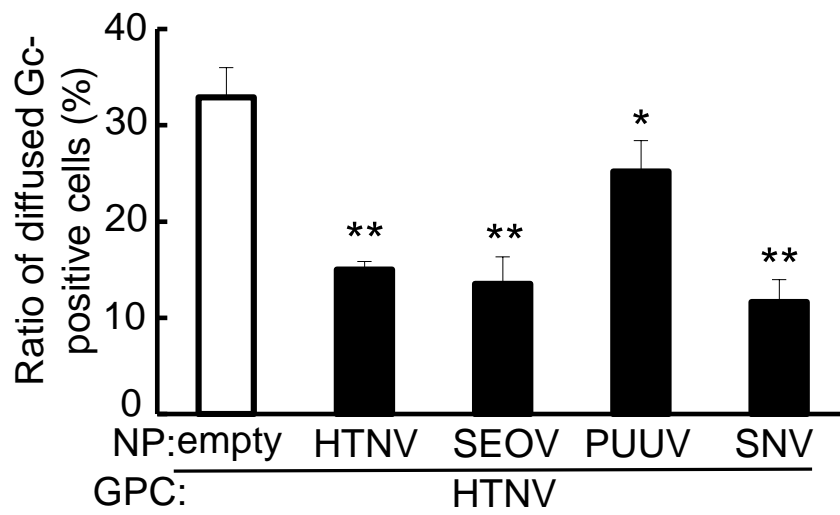


Fig. 4

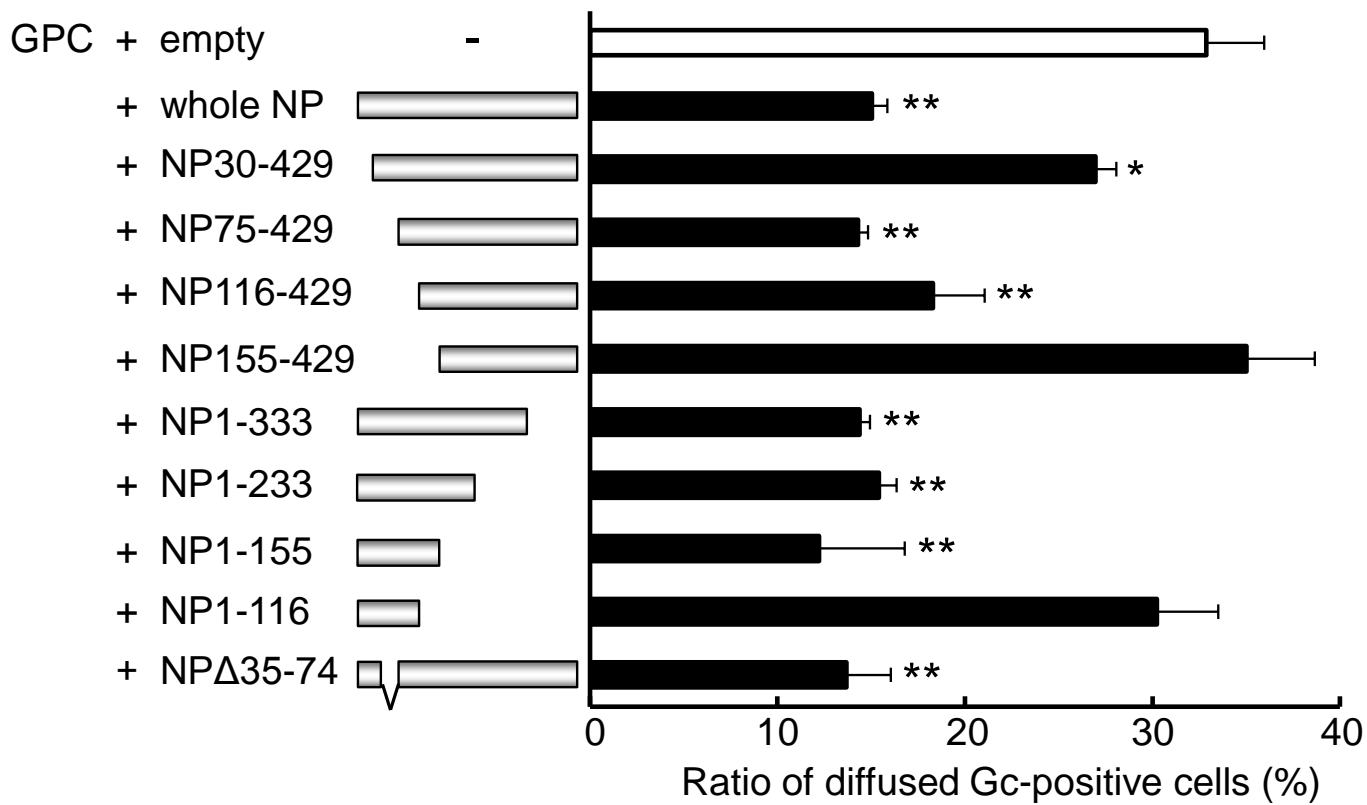


Fig. 5

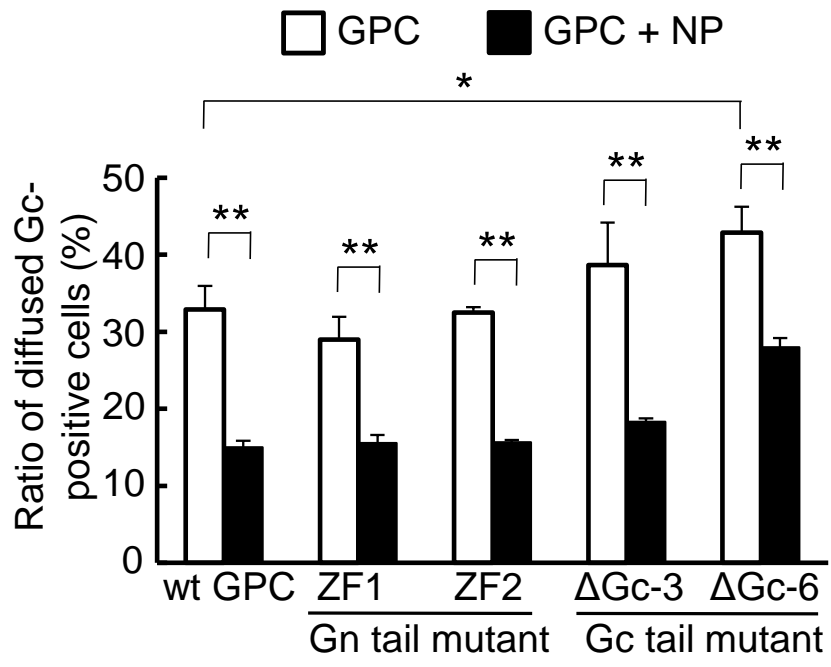
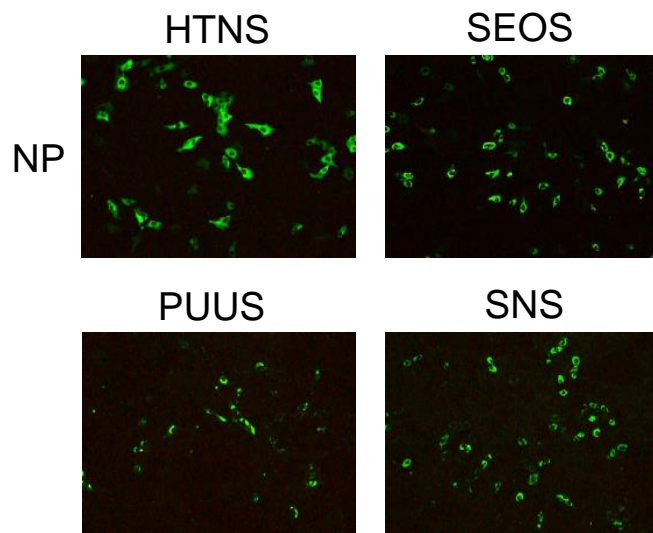


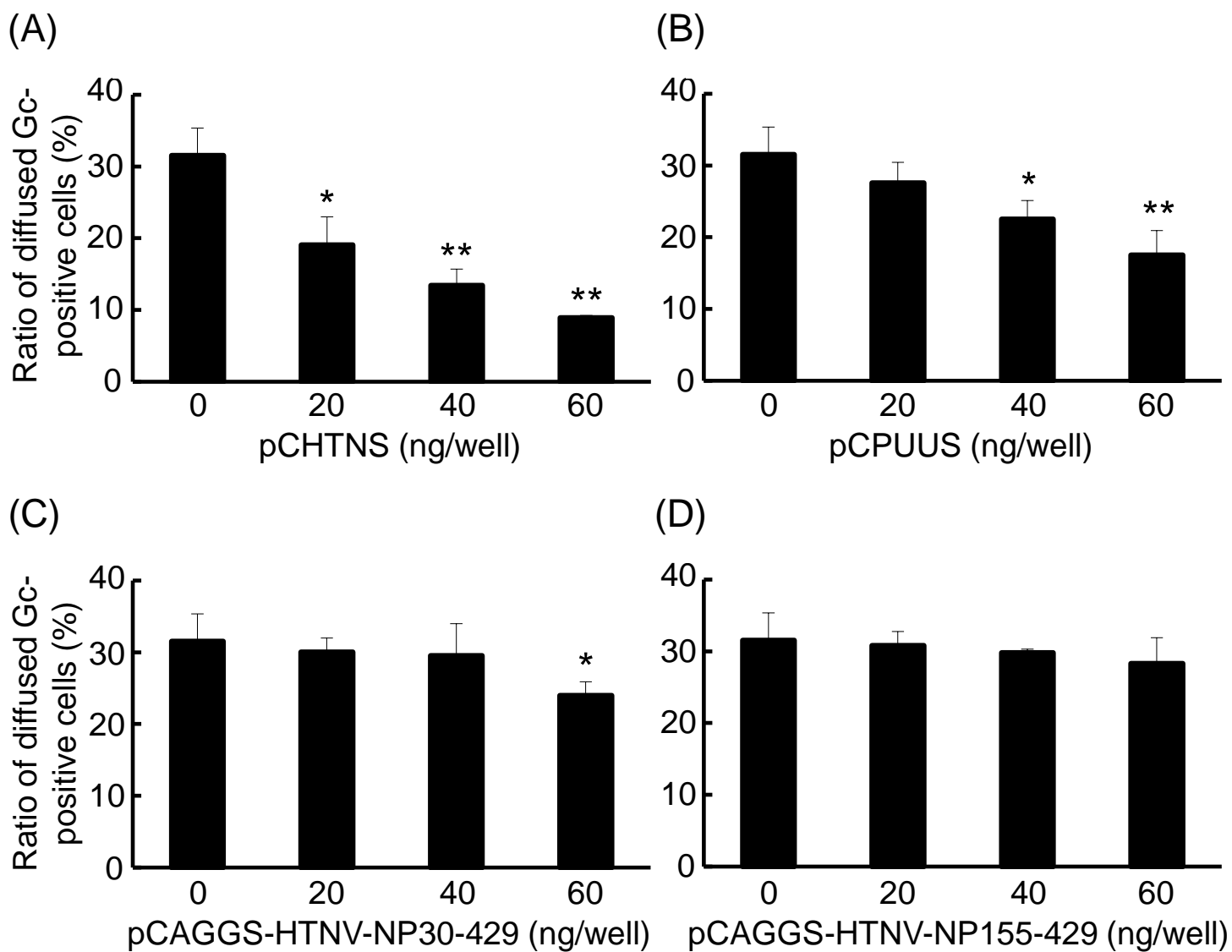
Fig. 6

Hantaan virus	TADWLSIIVYLTSFVVPILLKALYMLTTRGRQTTKDNKGT
Seoul virusT.....I.....S.....M
Thailand virusT.....I..I.....M
Dobrava virusV.....M
Saaremaa virusV.....M
Puumala virusYT.G..VIG.TI..I.....S.....V.E....
Topografov virusFT.G..IV..TL..I.....S.....V.E....
Khabarovsk virusFT.G..II..TL..I.....S.....V.E....
Tula virusF..GQ.I.G.ALA.I.....S.....I.E....
Prospect Hill virusK.GS.IIG.AL..I.....S.....V.E....
Isla Vista virusQ.GS.II..AL..I.....S.....V.E....
Sin Nombre virusK..GL.IL..AL..I.....S.....I.E....
New York virusKA.GM.IL..AI..I.....S.....V.E....
Rio Segundo virusR..GM.IL..TL..V.....S.....V.E....
El Moro Canyon virusK..GL.IL..TL..V.....S.....VQE....
Cano Delgadito virusKT.G..VLG.AI..I.....S.....V.E....
Andes virusKA.GA.ILG.AI..I.....S.....V.....
Laguna Negra virusKA.GA.ILG..I..I.....S.....V.E....
Rio Mamore virusKA.GA.ILG..I..V.....S.....V.E....
Black Creek Canal virusKA.GT.IL...L..V.....S.....V.E....
Bayou virusKA.G..IL...L..V.....S.....V.E....
Muleshoe virusKA.G..VL...L..V.....S.....V.E....
Thottapalayam virus	..N.GK.FE.ILTLTQVL...G..I.....S.....
	** * * * * ** ** * ** ** ** **

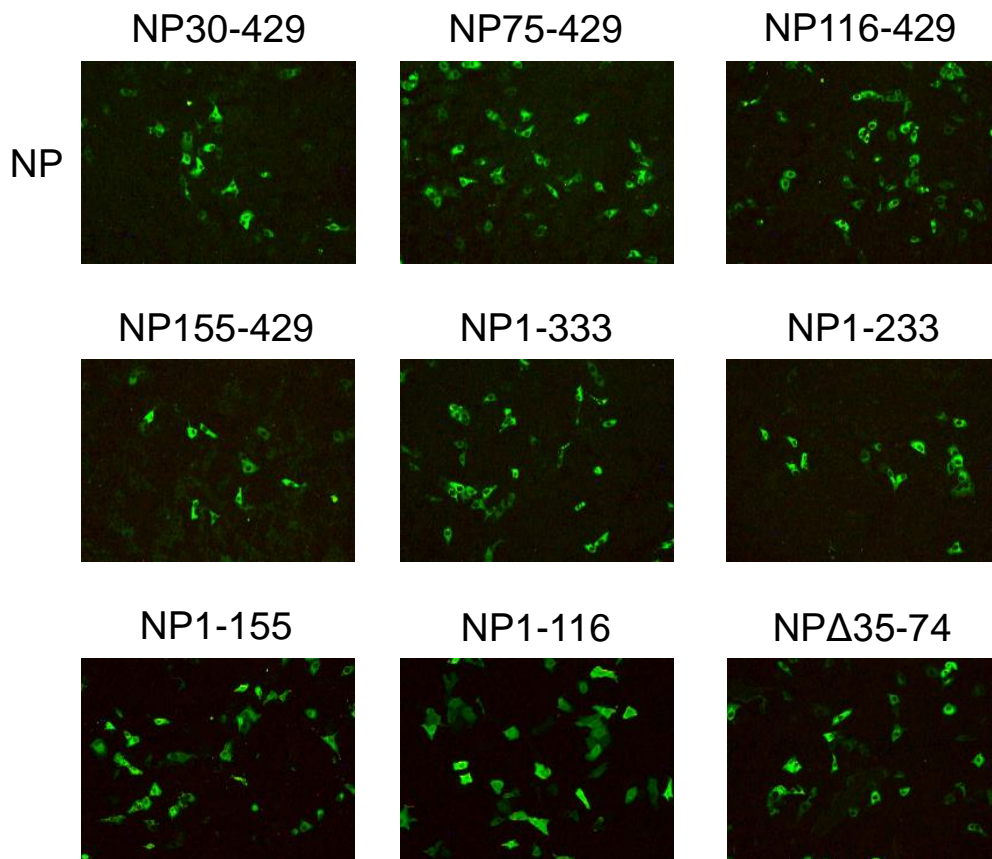
Fig. 7



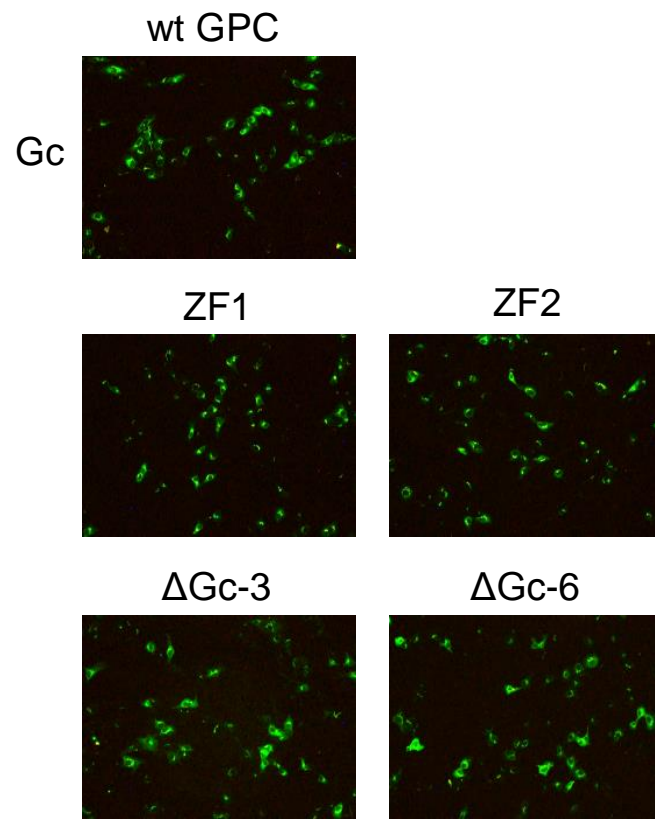
Supplementary figure 1



Supplementary figure 2



Supplementary figure 3



Supplementary figure 4